The ISME Journal (2007) 1, 517–531

www.nature.com/ismej

ORIGINAL ARTICLE

Phytoplankton carbon fixation gene (RuBisCO) transcripts and air-sea CO_2 flux in the Mississippi River plume

David E John[1], Zhaohui A Wang[1], Xuewu Liu[1], Robert H Byrne[1], Jorge E Corredor[2], José M López[2], Alvaro Cabrera[2], Deborah A Bronk[3], F Robert Tabita[4] and John H Paul[1]
[1]*College of Marine Science, University of South Florida, St Petersburg, FL, USA;* [2]*Department of Marine Sciences, University of Puerto Rico, Recinto Universitario de Mayagüez, Mayagüez, Puerto Rico;* [3]*Department of Physical Sciences, Virginia Institute of Marine Science, The College of William and Mary, Gloucester Point, VA, USA and* [4]*Department of Microbiology, The Ohio State University, Columbus, OH, USA*

River plumes deliver large quantities of nutrients to oligotrophic oceans, often resulting in significant CO_2 drawdown. To determine the relationship between expression of the major gene in carbon fixation (large subunit of ribulose-1,5-bisphosphate carboxylase/oxygenase, RuBisCO) and CO_2 dynamics, we evaluated *rbcL* mRNA abundance using novel quantitative PCR assays, phytoplankton cell analyses, photophysiological parameters, and pCO_2 in and around the Mississippi River plume (MRP) in the Gulf of Mexico. Lower salinity (30–32) stations were dominated by *rbcL* mRNA concentrations from heterokonts, such as diatoms and pelagophytes, which were at least an order of magnitude greater than haptophytes, α-*Synechococcus* or high-light *Prochlorococcus*. However, *rbcL* transcript abundances were similar among these groups at oligotrophic stations (salinity 34–36). Diatom cell counts and heterokont *rbcL* RNA showed a strong negative correlation to seawater pCO_2. While *Prochlorococcus* cells did not exhibit a large difference between low and high pCO_2 water, *Prochlorococcus rbcL* RNA concentrations had a strong positive correlation to pCO_2, suggesting a very low level of RuBisCO RNA transcription among *Prochlorococcus* in the plume waters, possibly due to their relatively poor carbon concentrating mechanisms (CCMs). These results provide molecular evidence that diatom/pelagophyte productivity is largely responsible for the large CO_2 drawdown occurring in the MRP, based on the co-occurrence of elevated RuBisCO gene transcript concentrations from this group and reduced seawater pCO_2 levels. This may partly be due to efficient CCMs that enable heterokont eukaryotes such as diatoms to continue fixing CO_2 in the face of strong CO_2 drawdown. Our work represents the first attempt to relate *in situ* microbial gene expression to contemporaneous CO_2 flux measurements in the ocean.
The ISME Journal (2007) **1,** 517–531; doi:10.1038/ismej.2007.70; published online 30 August 2007
Subject Category: geomicrobiology and microbial contributions to geochemical cycles
Keywords: phytoplankton productivity; carbon dynamics; diatoms; *Prochlorococcus*; nutrient plumes; RNA

Introduction

Perhaps the least understood components of the global carbon cycle are those that involve the coastal ocean. About half of the approximately 115 pg of carbon fixed by autotrophs annually is taken in by marine organisms (Behrenfeld *et al.*, 2001). It is estimated that about 30% of anthropogenic CO_2 emissions are absorbed into the oceans (Sabine *et al.*, 2004) and the ocean margins have recently been shown to take up about 20% of this anthropogenic CO_2 (Thomas *et al.*, 2004). Coastal seas, estuaries and river plumes are a fundamental part of the global carbon cycle because they link terrestrial, oceanic and atmospheric carbon reservoirs. River-dominated ocean margins are the most important class of margins in terms of their impact on carbon sequestration (Green *et al.*, 2006). In addition, river-born nutrients yield the highest rates of primary production in the biosphere (Dagg *et al.*, 2004).

The Mississippi is the Earth's seventh largest river by discharge, and its outflow into the Gulf of Mexico creates a plume of elevated phytoplankton abundance in the stratified and otherwise oligotrophic Gulf waters. While Mississippi River water entering the Gulf of Mexico has very high dissolved inorganic carbon (DIC) concentrations and is believed to be a

Correspondence: DE John, College of Marine Science, University of South Florida, 140 7th Ave. S, St Petersburg, FL 33701, USA.
E-mail: djohn@marine.usf.edu
Received 18 April 2007; revised 9 July 2007; accepted 9 July 2007; published online 30 August 2007

source of atmospheric CO_2, the region of mixing with oceanic water fosters high levels of primary productivity and inorganic carbon uptake, resulting in an area of estimated CO_2 influx to the surface ocean (Cai, 2003; Green *et al.*, 2006; Lohrenz and Cai, 2006). Evidence indicates maximum phytoplankton biomass and primary production occurs at intermediate salinities (20–30) in the Mississippi River plume (MRP), while productivity is light-limited in very low salinity water and nutrient-limited at the edges and outside the plume, where seawater CO_2 partial pressure (pCO_2) increases and approaches equilibrium with the atmosphere (Lohrenz *et al.*, 1999). Productivity rates of the MRP are among the highest of river-influenced continental shelf systems (Cai, 2003). Phytoplankton blooms composed largely of chain-forming diatoms have been documented (Bode and Dortch, 1996), particularly in the low-salinity plume water. Picoplankton such as *Synechococcus* and picoeukaryotes, while generally still in greater abundance than larger phytoplankton in the plume, appear to become relatively more prominent in regions with salinity around 30, as plume waters mix with the Gulf of Mexico, while *Prochlorococcus* spp. are present in high numbers outside the plume (salinity $\sim$35) in oligotrophic Gulf of Mexico waters (Jochem, 2003; Liu *et al.*, 2004; Wawrik and Paul, 2004).

From a molecular standpoint, by far the most common mode of inorganic carbon entry into the biosphere is via the enzyme ribulose-1,5-bisphosphate carboxylase/oxygenase (RuBisCO). RuBisCO sequences are somewhat conserved across evolution yet still exhibit sufficient variation to enable phylogenetic discrimination. Most phytoplankton contain the form I type of RuBisCO, including marine α-cyanobacteria such as *Synechococcus* and *Prochlorococcus* (form IA), chlorophytes and β-cyanobacteria (form IB), and chromophytic algae such as diatoms and prymnesiophytes (form ID) (Tabita, 1995, 1999) Although regulation of RuBisCO activity is complex (Hartman and Harpel, 1994), most phytoplankton actively transcribe their large subunit genes (*rbcL*) daily, making *rbcL* mRNA a good molecular indicator of carbon fixation potential (Pichard *et al.*, 1996; Paul *et al.*, 2000b). Much work has focused on the measurement of *rbcL* mRNA transcript abundances to gain information about the occurrence and phylogenetic diversity of active carbon-fixing organisms in the marine environment (Wyman *et al.*, 2000; Paul *et al.*, 2000a; Wawrik *et al.*, 2003, 2004; Corredor *et al.*, 2004). Our previous work on RuBisCO gene expression and phytoplankton dynamics in the Gulf of Mexico has revealed elevated form IA *rbcL* transcript and primary productivity associated with offshore or distal plume environments (Paul *et al.*, 2000a; Wawrik *et al.*, 2003, 2004). However, this work has largely excluded the most biologically active waters of the MRP immediately to the south and west of the delta, where other research has demonstrated pCO_2 gradients that favor carbon flux to surface waters whereby the plume may act as a carbon sink.

The analysis of *rbcL* transcript abundances is important for giving not only an indication of presence but also relative *rbcL* gene expression levels from phytoplankton populations sampled. Following development of a quantitative reverse transcription PCR method for quantifying *rbcL* mRNA (Wawrik *et al.*, 2002), we have recently described a suite of quantitative reverse transcription PCR assays to quantify *rbcL* RNA from *Synechococcus*, high-light *Prochlorococcus*, haptophytes, and the heterokont group from the previously described assay which encompasses diatoms, pelagophytes, pinguiophytes and dictyochophytes (silicoflagellates) (John and Paul, 2007). These groups were targeted initially because *rbcL* mRNA clone library analysis from the Gulf of Mexico identified diatoms, prymnesiophytes, α-*Synechococcus*, and *Prochlorococcus* to be the dominant-active carbon fixers in plume and oligotrophic waters (Wawrik *et al.*, 2003; Wawrik and Paul, 2004).

The inverse correlation between phytoplankton biomass (as chlorophyll-*a*) and surface CO_2 levels in ocean margin environments has been demonstrated recently in a coastal area of the Mediterranean Sea (Huertas *et al.*, 2005). Still, data on the relationship between phytoplankton communities and pCO_2 levels of the surface oceans are lacking, particularly with respect to which members of the phytoplankton community can be the most important in effecting CO_2 drawdown. In the current study, we addressed the question of which major phytoplankton groups are present and active with respect to CO_2 dynamics in the MRP and northern Gulf of Mexico. We employed a number of analyses, including *rbcL* mRNA quantification using new real-time PCR assays and form-specific hybridization probes, phytoplankton cell abundances by flow cytometry and microscopic counts, primary productivity measurements, and size fractionation of samples along with underway and discrete inorganic carbon measurements to answer this question.

Methods

RNA sampling and rbcL *gene transcript quantification*
Sampling was performed aboard the *R/V Pelican* in July 2005. For mRNA, seawater samples (450–750 ml) were collected from 3 m depth using an electric submersible pump (Rule, White Plains, NY, USA). Phytoplankton were filtered onto 0.45 μm Durapore HVLP filters (Millipore, Billerica, MA, USA) and filters were stored in 2 ml polypropylene cryotubes previously filled with 0.3 ml of muffled 200 μm low-protein-binding zirconium oxide grinding beads (OPS Diagnostics, Bridgewater, NJ, USA) and 750 μl RLT buffer (Qiagen, Valencia, CA, USA) with 10 μl/ml β-mercaptoethanol (Sigma, St Louis,

MI, USA). Samples were frozen and stored in liquid nitrogen for the duration of the cruise, and stored at −80°C upon return to the lab until analysis.

RNA purification was performed in the lab using the RNEasy extraction kit (Qiagen) on a vacuum manifold with on-column DNA digestion using RNAse-free DNAse (Qiagen) according to manufacturer's instructions. Columns were rinsed twice using 750 µl RPE buffer rather than the recommended 500 µl to ensure adequate removal of guanidinium-containing buffers RW1 and RLT from the sides and ledge in the columns. Columns were centrifuged at 16 100 *g* for 2 min to dry following RPE rinses. RNA was eluted using 50 µl room temperature RNAse-free H_2O. Purified RNA was diluted up to 10-fold to reduce the possibility of PCR inhibition by compounds co-purified with the RNA. PCR oligonucleotides employed were as reported previously (John and Paul, 2007; Supplementary data). Reactions were performed using the Taqman One-step RT-PCR master mix kit (Applied Biosystems, Foster City, CA, USA) on an ABI Prism 7700 Sequence Detector real-time PCR instrument (Applied Biosystems). PCR reactions were composed of primers at concentrations of 400 nM each, with primers pooled in assays with multiple primers (thereby giving total concentrations ranging from 400 nM to 2 µM, depending on the assay), probes at concentrations of 125 nM for single-probe assays and 75 nM each for two-probe assays (150 nM total), 1.25 µl Multiscribe reverse transcriptase (from Taqman kit), 25 µl 2 × Taqman master mix, 10 µl template in RNAse-free H_2O, and the balance to 50 µl with RNAse-free H_2O. Thermocycling conditions for heterokonts were as follows: 45°C hold for 30 min, 95°C hold for 10 min, then 40 cycles of 95°C for 20 s, 52°C for 60 s and 72°C for 60 s; haptophytes, high-light *Prochlorococcus* and *Synechococcus* were performed at 45°C hold for 30 min, 95°C hold for 10 min, then 40 cycles of 95°C for 20 s, 54°C for 60 s and 72°C for 60 s.

Data were analyzed using the Sequence Detection Systems software version 1.9 (Applied Biosystems). Standard curve reaction templates were created from our clone libraries of *rbcL* genes (Wawrik and Paul, 2004) and reactions consisted of a pool of three *in vitro* transcripts from the target clade. Standard curves encompassing five orders of magnitude were generated for each PCR run. Results were interpreted in terms of mass of transcript RNAs made using the Quant-iT Ribogreen kit (Invitrogen, Carlsbad, CA, USA). Each RNA extraction was analyzed for all four assays by performing reactions in two groups according to annealing temperature and holding the extracted RNA on ice during the interim while the first round of PCR was running. Average values for the respective groups were calculated using data from two separate samples.

RNA extraction and sample analyses for dot-blot hybridization were performed as has been described previously (Wawrik *et al.*, 2003; Corredor *et al.*, 2004). Briefly, RNA was purified using RNeasy columns and dot blots were quantitatively analyzed using antisense ^{35}S-labeled probes for form IA, form IB and form ID *rbcL.* Quantitative standard curves were created from dilutions of sense *in vitro* transcripts made from the respective probe template sequence. Standard curve dilutions were blotted in the same manner as environmental samples and probed with respective riboprobes along with environmental sample blots. Samples were analyzed in duplicate.

Productivity and photophysiology

For photophysiology analysis, samples taken in Teflon-lined Niskin bottles were immediately transferred to 1-liter light-shielded, acid-washed polyethylene bottles. Samples of 650 ml were spiked with 0.108 mCi of ^{14}C-bicarbonate (Amersham Biosciences, Piscataway, NJ, USA). Aliquots (40 ml) of spiked water were transferred to 40-ml borosilicate EPA vials and incubated in a photosynthetron apparatus (CHPT Mfg, Georgetown, DE, USA) at *in situ* temperature and at irradiances ranging from 0 (dark sample) to 1000 µE m^{-2} s^{-1}. Time-zero sample blanks were immediately filtered before commencement of incubation. Following incubation (1–2 h), samples were sequentially filtered onto 2 and 0.2 µm 25-cm membrane filters and treated with 250 µl 10% HCl to drive off unfixed [^{14}C]bicarbonate. After 24 h, 10 ml of scintillation fluid was added, and sample radioactivity was determined by liquid scintillation counting in the channels ratio mode. The resulting data were plotted in PE (productivity vs irradiance) curves. The biomass (chlorophyll-*a*) normalized photosynthetic parameters α^B (light-limited slope), P^B_{max} (light saturated rate) and β^B (photoinhibition slope) were computed using the exponential formulation of Platt *et al.* (1990). Samples for chlorophyll-*a* analysis (200 ml) were sequentially filtered through 2 and 0.2 µm membrane filters, frozen in liquid nitrogen and then ground in 5 ml 90% acetone solution in a Potter–Elvejhm grinder using a glass fiber filter to assist in cell disruption. Fluorescence analysis was performed following the method of Welschmeyer (1994).

Carbonate chemistry analyses

Shipboard CO_2-parameter analyses were performed using an automated flow-through multiparameter instrument (Wang *et al.*, 2007). The instrument takes complete measurement of air pCO_2, seawater pCO_2, DIC and pH every 7 min. Detailed procedures of the spectrophotometric measurements of these carbon parameters have been presented previously (Byrne *et al.*, 2002; Wang *et al.*, 2007). Briefly for pCO_2, an internal alkalinity standard with a sulfonephthalein indicator (phenol red) is enclosed inside a liquid core waveguide made of Teflon AF 2400 capillary tubing (DuPont, Wilmington, DE, USA), which

forms the long pathlength spectrophotometric cell during measurements. CO_2 samples are directed to flow surrounding the liquid core waveguide, which also serves a CO_2-permeable membrane. The internal standard indicator solution reaches CO_2 equilibrium with sample across the liquid core waveguide, solution pH is measured with a spectrophotometer, and pCO_2 is then calculated. The internal indicator solution is renewed for each measurement. pCO_2 measurements are calibrated against known pCO_2 gas standards. For DIC measurements, sampled seawater is first acidified using 3 N HCl to convert all inorganic carbon species to CO_2, which is subsequently measured using bromocresol purple as the indicator. DIC measurements are calibrated with Certified Reference Material (CRM) from Dr AG Dickson at the Scripps Institution of Oceanography (La Jolla, CA, USA). All measurements and calibrations are conducted at a constant temperature (25°C) using a water thermostat. The system is also equipped with a pressure gauge for measurement of atmospheric pressure and a CTD for measurements of temperature and salinity of water samples. The entire system and its measurement sequence are fully automatic and controlled by a PC through a custom interface. The measurement precisions are ± 1 μatm for water and atmospheric pCO_2, and ± 2 μmol kg^{-1} for DIC.

During field measurements, seawater samples were pumped into the ship using an on-board water pump with an inlet about 3 m below the surface. The multiparameter CO_2 system withdrew water from the underway stream through a peristaltic pump. Atmospheric sample air was pumped from the front of the ship about 10 m above sea surface and was directed to the underway CO_2 system. Results of seawater pCO_2 measured at 25°C were corrected to the field temperature based on thermodynamic calculation of the carbonate system. During the survey, calibrations of pCO_2 and DIC were conducted occasionally to assure that no drift occurred. For hydrographic casts and time series monitoring, discreet samples of DIC were collected in stoppered glass bottles free of headspace and preserved with saturated $HgCl_2$. These DIC samples were subsequently measured on board using the underway CO_2 system described above.

Phytoplankton cell counts

Samples for phytoplankton cell counts were concentrated by reverse filtration (Dodson and Thomas, 1978) using 1 μm pore-sized polycarbonate filters. Typically, 400 ml was concentrated to approximately 25 ml of which 5 ml was counted on a Zeiss inverted microscope following the procedures outlined by Hasle (Dodson and Thomas, 1978). The entire chamber was counted at 100× for larger species while two to four chamber transects were counted at 400× for smaller species. Species identifications were based on descriptions in the Tomas manual of phytoplankton identification (Tomas, 1997). Samples for flow cytometry were processed in the lab of Lisa A Campbell at Texas A and M University according to protocols described previously (Campbell, 2001).

Diel drift study

A Lagrangian drift study was performed to measure diel changes in *rbcL* transcript abundances and the other parameters. A drogued drift buoy was deployed and followed for over 24 h. Samples from 3 m were taken every 4 h as described above for RNA analyses and photophysiological parameters. Surface water pCO_2 and DIC were also measured using the underway CO_2 system described above.

Results

Surface seawater characteristics in study region

Locations of sampling stations are shown in Figure 1 and Table 1. Station 1 was just off the Florida Shelf in oligotrophic waters (not shown in Figure 1). Stations 3, 4 and 6 were in the area of greatest river influence, evidenced by satellite ocean color, salinity and chlorophyll-*a*. Stations 6 and 7A–F were part of a Lagrangian study, thus were rather close in proximity. The salinity of sampling stations ranged from 30.1 to 35.9 (Table 1). Satellite-estimated chlorophyll content of surface water within the sampling area (Figure 1a) indicates highly productive waters were present at the time of sampling. Seawater DIC and pCO_2 for all stations ranged from 1911 to 2031 μmol kg^{-1} and 188–437 μatm, respectively; both generally increased with salinity, although the station with lowest pCO_2 (Station 4) did not have lowest DIC concentrations. Atmospheric pCO_2 over sampling stations (corrected to 100% humidity) was fairly constant at 370 ± 3 μatm. Underway carbon measurements were used to chart spatial dynamics of surface water pCO_2 (Figure 1b). Low seawater pCO_2, well below atmospheric levels, was observed in the plume region, resulting in an area of estimated CO_2 drawdown (Stations 3–7). Conversely, in the oligotrophic waters outside the MRP, a small degree of CO_2 efflux was observed (Stations 1, 2 and 8).

These parameters allow the categorization of sampling stations into two basic surface marine regimes (Figure 2): (1) a 'plume' area characterized by lower salinity from 30 to 32, surface pCO_2 from under 200 to just over 300 μatm and CO_2 flux into the surface ocean from the atmosphere, elevated chlorophyll-*a*, and elevated maximum photosynthetic rate (P_{max}); and (2) the open, oligotrophic Gulf of Mexico with salinity over 34, pCO_2 over 400 μatm, and much lower chlorophyll-*a* and P_{max} measurements. The size distribution of photosynthetic cells, indicated by chlorophyll-*a* content, also varied between these two regimes (Figure 2b); larger cells

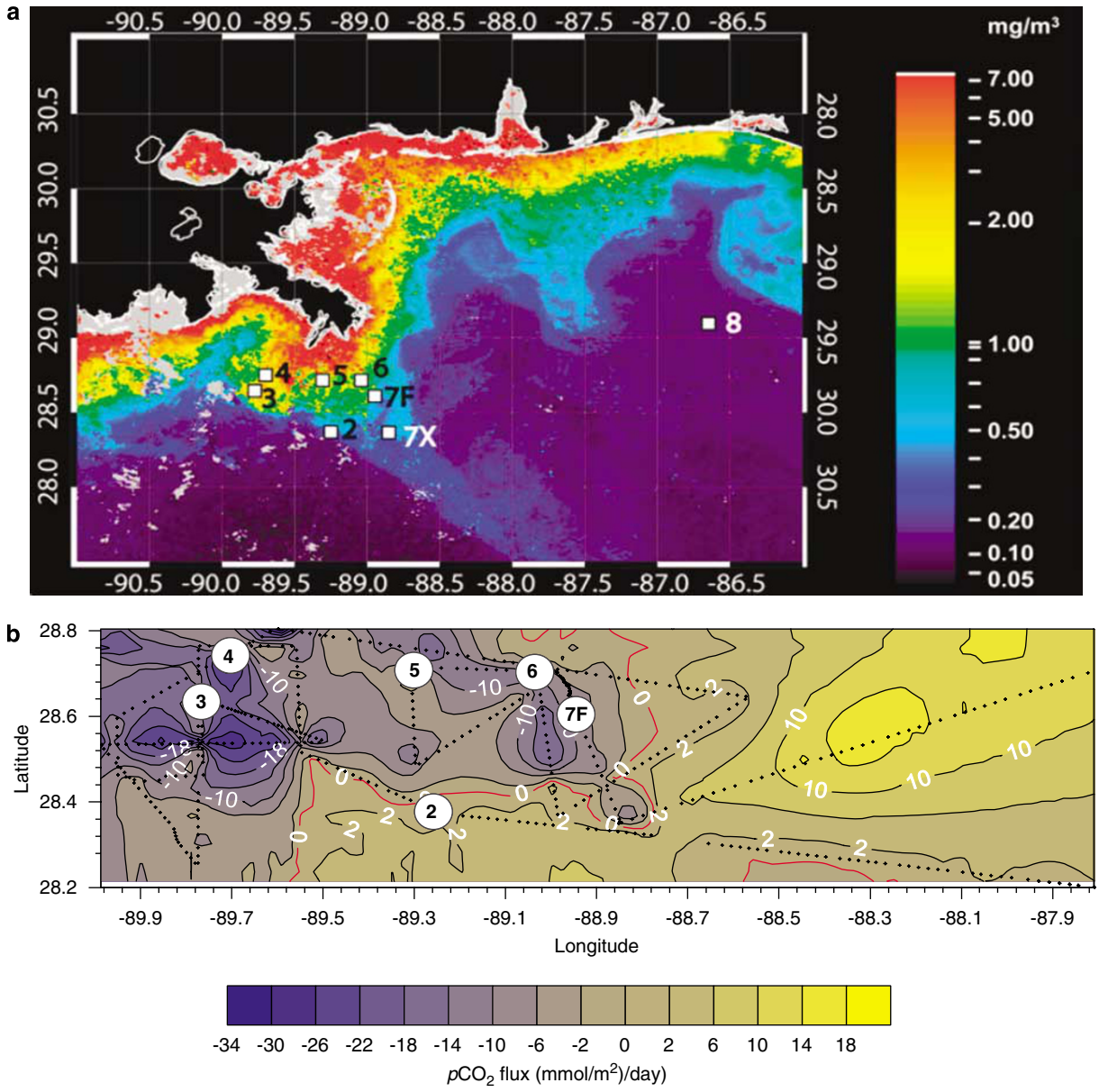

Figure 1 (**a**) Composite SeaWiFS image of estimated surface chlorophyll-*a* concentrations during cruise dates in July 2005. Sampling stations are shown, with 1 oligotrophic station out of view (Station 1). Station 7 × was not sampled for data reported here. (**b**) Estimated CO_2 flux (based on Wanninkhof parameterization (Wanninkhof, 1992)) over the MRP area, showing sampling sites and cruise track within or near the plume. The negative sign of numbers in the lower panel indicates the direction of pCO_2 flux is from atmosphere to surface ocean. Two sampling sites far outside the MRP are not shown (Stations 1 and 8). MRP, Mississippi River plume.

(>2 μm) contained the bulk of total chlorophyll-*a* within the plume, while outside it the photosynthetic biomass was dominated by picoplankton <2 μm.

Phytoplankton cell numbers

Two types of phytoplankton cell count data were obtained: picophytoplankton (*Prochlorococcus*, *Synechococcus* and picoeukaryotes) were enumerated by flow cytometry, from both the <2 μm and whole (unfiltered) size fractions, while microphytoplankton such as diatoms, dinoflagellates, *Trichodesmium* and microflagellates (which were not differentiated into auto- or heterotrophic organisms, see Methods) were counted by light microscopy from preserved samples. Figure 3 shows microplankton and picoplankton (whole fraction) counts as a function of surface water pCO_2. *Synechococcus* cells were in greatest abundance in the plume, and ranged from about $1 \times 10^8\,l^{-1}$ to a peak of over $6 \times 10^8\,l^{-1}$ at Station 7F at the end of the diel study. *Synechococcus* cell abundance in high pCO_2, oligotrophic waters was <3% of the maximum abundance we measured (Figure 3a). *Prochlorococcus* were more numerous far outside the plume (Stations

Table 1 Locations of sampling stations from *R/V Pelican* cruise from 14 to 19 July, 2005, and accompanying DIC and productivity measurement values

Station	*Salinity*	*Latitude*	*Longitude*	*Sampling time (EDT) (hours)*	*DIC (μmol/kg)*	*pCO_2 (μatm)*	*pCO_2 air (μatm)*	*Chlorophyll-a ($\mu g\,l^{-1}$)*	*P_{max} ($\mu g\,C\,l^{-1}\,h^{-1}$)*
4	30.1	28.750 N	89.700 W	1530	1980	188	367	2.10	7.15
3	30.9	28.645 N	89.775 W	0915	1911	218	373	1.82	4.51
6	31.6	28.715 N	89.040 W	1245	1953	293	369	1.86	2.81
7A	31.3	28.691 N	88.998 W	1841	1930	267	366	1.73	5.94
7B	31.4	28.691 N	88.975 W	2230	1940	272	367	1.68	2.81
7C	31.5	28.657 N	88.960 W	235	1941	282	368	1.54	4.94
7D	32.0	28.633 N	88.948 W	0639	1949	303	368	0.97	0.76
7E	32.0	28.620 N	88.947 W	1025	1955	306	369	0.55	5.71
7F	31.8	28.610 N	88.947 W	1433	1956	310	372	0.80	2.38
5	32.0	28.715 N	89.307 W	0908	1949	283	371	1.64	6.91
2	34.2	28.385 N	89.250 W	1015	2013	412	368	0.27	0.99
8	35.7	29.096 N	86.647 W	0900	2023	430	370	0.14	0.70
1	35.9	28.098 N	85.389 W	0800	2031	437	372	ND	ND

Abbreviation: DIC, dissolved inorganic carbon.
All data reported were taken from samples at a depth of 3 m to reflect surface water characteristics. Atmospheric pCO_2 values were corrected for 100% humidity. ND: not determined, samples were not analyzed for specified parameter at that station. Stations listed in order of increasing salinity except for Stations 6–7F, which were part of a diel drift study.

1 and 8), reaching a maximum of $8 \times 10^7\,l^{-1}$, but were still present in the plume at about one-third of their highest concentrations. Picoeukaryote cell concentrations were much greater in low pCO_2 water. All three picoplankton classes were primarily in the $<2\,\mu m$ fraction, with the average ratio of cells $<2\,\mu m$ being 93% for *Prochlorococcus* and 100% for *Synechococcus* and picoeukaryotes, but showing no clear relationship to sampling location (Supplementary data). All three picoplankton classes were in greater abundance than diatom cells, which were the most numerous larger phytoplankton in the plume except at Station 5 (where they were in equal abundance to microflagellates, Figure 3b, note difference in scale). Of the diatoms in the plume area (pCO_2 below $\sim 300\,\mu atm$), 96–99% were tentatively identified as *Pseudo-nitschia* (G Vargo, personal communication). Dinoflagellates were also dramatically greater in the plume than outside it, and the decrease of pCO_2 with increasing diatom and dinoflagellate numbers is visible in the scatterplot of Figure 3b. In oligotrophic water, diatoms were far less abundant, and were not found at Station 1. Except at Station 5, microflagellates numbers were fairly consistent within and outside the plume.

RuBisCO RNA concentrations

RuBisCO RNA transcripts quantified by quantitative PCR (qPCR) were averaged for each group for the two oceanic regions (Figure 4a), from the whole and size-fractionated samples. *rbcL* RNA from the heterokont group was in greatest abundance in plume stations (Stations 3–7, Figure 4a, also Supplementary data). Again, the heterokont group does not encompass all heterokonts, but rather a group with related *rbcL* genes primarily consisting of diatoms (Bacillariophyta), and including pelagophytes (Pelagophyceae), pinguiophytes (Pinguiophyceae), and some silicoflagellates (Dictyochophyceae). Whole-fraction heterokont *rbcL* transcripts were approximately $10\times$ more abundant than the other analyzed groups in the plume, and $50\times$ more abundant than from the $<2\,\mu m$ fraction (Figure 4a). High-light *Prochlorococcus rbcL* RNA concentrations were very low in the plume, but increased in non-plume stations (Stations 1, 2 and 8) to equal abundance essentially with the other four groups ($\sim 10\,pg\,l^{-1}$). Picocyanobacterial (*Prochlorococcus* and *Synechococcus*) *rbcL* RNA occurrence was nearly equal between the whole and $<2\,\mu m$ fractions, indicating again that picocyanobacteria cells were in the $<2\,\mu m$ fraction.

Results of diel sampling from this study (Figure 4b and Supplementary data) and from our and others' previous work (Pichard *et al*., 1996; Paul *et al*., 1999, 2000b; Wyman, 1999) demonstrate that much of the cellular RuBisCO RNA pools fluctuate daily, with peak concentrations tending toward early morning hours. Diel variability here was most pronounced for the heterokont group *rbcL* RNA (Figure 4b), with the minimum concentration only about 10% of the maximum (other *rbcL* clades' diel results shown in Supplementary data). With the exception of Station 4 in the plume and three diel time points, samples were collected between 0600 and 1300 Eastern Daylight Time (Table 1). The averages in Figure 4a omit these stations so that samples are better constrained with respect to time and differences between water masses are more defined. Indeed, RNA concentrations from Station 4 (sampled 15:30) were relatively lower than other plume stations for all analyzed groups (station-by-station *rbcL* RNA values are shown in Supplementary data).

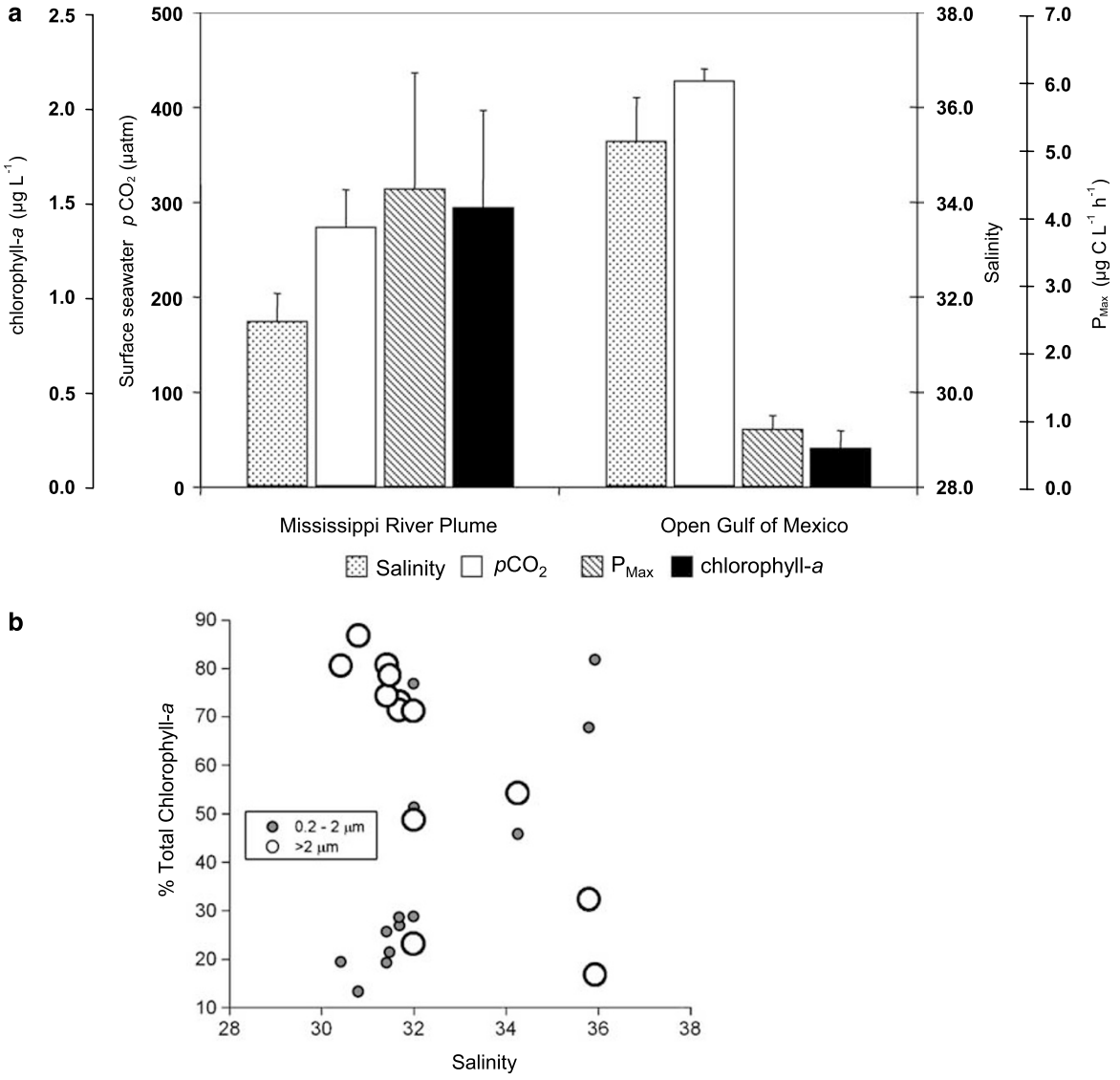

Figure 2 (**a**) Mean values of surface (3 m) salinity, pCO_2, P_{max} (maximum photosynthetic potential) and chlorophyll-*a* in plume and open Gulf of Mexico stations. Error bars indicate standard deviation. Plume stations were defined as having salinity 30–32, open ocean stations defined as having salinity >34. (**b**) Relative distribution of chlorophyll-*a* between cell size fractions above and below 2 µm diameter with respect to salinity. At lower salinity stations, chlorophyll-*a* was predominantly in cells >2 µm, conversely most chlorophyll-*a* was in picoplankton <2 µm at open ocean, high salinity stations.

We also made measurements of *rbcL* RNA concentrations using dot-blot hybridization with radiolabeled riboprobes consistent with previous studies on RuBisCO RNA in the marine environment (Supplementary data). There was good relative agreement between heterokont *rbcL* RNA measured via PCR and form ID *rbcL* RNA by hybridization, although PCR-derived RNA concentrations were somewhat greater. However, there was poor agreement in the relative trends between stations when comparing *Synechococcus* or *Prochlorococcus* PCR values and form IA RNA hybridization values. Rather, forms IA and IB hybridization values paralleled each other closely.

Data comparisons and correlations

To determine which parameters covaried, Pearson correlation coefficients were determined for the many parameters measured at the various stations. The most salient correlation analyses are shown in Table 2. For *rbcL* mRNA concentrations, only samples taken from 0600 to 1300 were considered, due to the strong diel periodicity in mRNA message levels we observed.

Heterokont *rbcL* RNA measured by PCR and microscopic cell counts of diatoms were highly correlated, as were heterokont *rbcL* RNA and the sum of diatom and microflagellates. These relationships are documented graphically in Figure 5 for emphasis. While a strong relationship existed

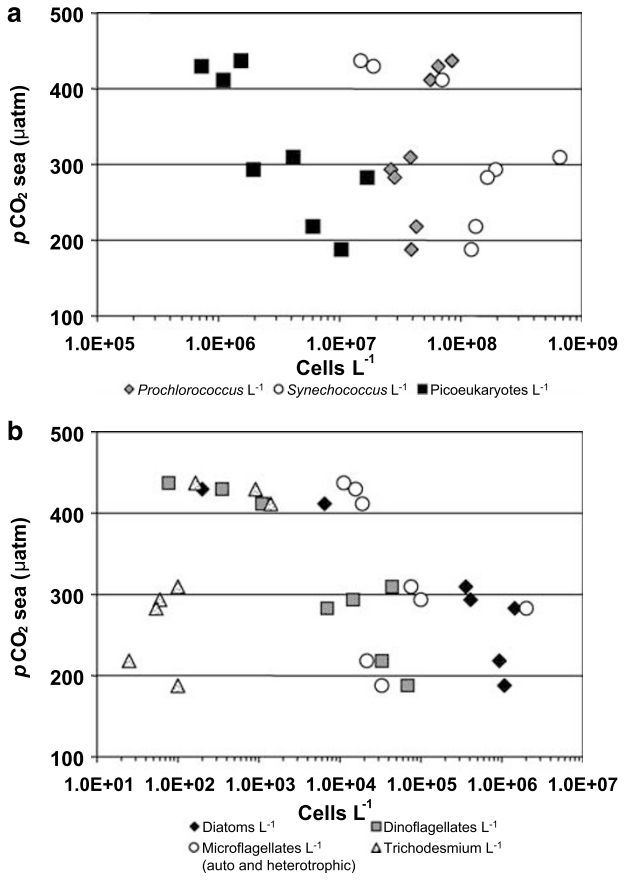

Figure 3 (**a**) Cell counts of picoplankton derived from flow cytometry vs surface pCO_2, showing *Prochlorococcus*, phycoerythrin-containing *Synechococcus* and picoeukaryotes. (**b**) Microplankton counted by light microscopy, showing diatoms, combined auto- and heterotrophic microflagellates, dinoflagellates and *Trichodesmium*. Note difference in scale between 3A and 3B. *Synechococcus* were the most abundant cell type throughout plume-influenced waters, but were outnumbered by *Prochlorococcus* at stations with salinity >35. Diatoms were the most abundant microplankton type in plume stations except at Station 5, but not observed from Station 1 samples.

between diatom cell counts and heterokont *rbcL* RNA overall, the relationship weakens in very oligotrophic water (Stations 1 and 8) where diatoms were undetected at Station 1 (approximately <1 per 80 ml or 13 per l) and only 200 cells l^{-1} at Station 8, yet heterokont *rbcL* RNA was still present. Since the heterokont qPCR assay also detects *rbcL* transcripts from pelagophytes (some of which are flagellates, for instance *Pelagomonas*) and silicoflagellates (dictyochophytes), it is likely that these organisms made up a larger or the entire portion of quantified heterokont *rbcL* RNA in waters where diatoms were largely absent. Indeed, the slope of the regression on heterokont *rbcL* RNA and the sum of diatom and microflagellate cells reveals a nearly 1:1 relationship on a logarithmic scale (appropriate considering the enormous scale of variability), so it is also possible a significant portion of the microflagellates in oligotrophic water were pelagophytes or silicoflagellates. In contrast, Figure 5c shows a large spread in abundance of high-light *Prochlorococcus rbcL* RNA but a relatively small range of *Prochlorococcus* cells enumerated by flow cytometry. The values of *rbcL* RNA below $\sim 1 \times 10^{3.5}$ fg l^{-1} all were from plume samples, while those greater than this were from the open Gulf of Mexico.

Correlations between diatoms or microflagellates and form ID *rbcL* RNA by hybridization were less robust, with *R*-values of around 0.7 (data not shown). The picoeukaryotes, which were primarily in the <2 µm size fraction, were not well correlated to the <2 µm fraction heterokont *rbcL* RNA, and were only moderately correlated to haptophyte *rbcL* RNA (<2 µm; Table 2). These picoeukaryotes may be any of a number of different photosynthetic organisms, including prasinophytes (which have form IB RuBisCO and were not specifically targeted with real-time PCR), but it does not appear a large portion of them were chromophytes targeted by our real-time PCR assay.

Chlorophyll-*a* and P_{max} correlation to *rbcL* RNA were strongest for the heterokont group; P_{max} also strongly correlated with diatom cell numbers. Relationships between salinity and *rbcL* RNA concentrations revealed high-light *Prochlorococcus rbcL* RNA to be positively correlated to salinity, and heterokont *rbcL* RNA to be negatively correlated. Surface pCO_2 and DIC were positively correlated with salinity and negatively correlated with chlorophyll-*a*. P_{max} also was negatively correlated to pCO_2; although less robust than salinity and chlorophyll, the regression is significant at $P<0.01$.

From the PCR-derived *rbcL* RNA concentrations, heterokont *rbcL* and high-light *Prochlorococcus rbcL* RNAs both had strong correlations to pCO_2 (and DIC, not shown), with heterokont values negatively correlated and *Prochlorococcus rbcL* RNA positively correlated. Diatom cell abundance also had a significant negative correlation to pCO_2, while *Prochlorococcus* cells did not. *Synechococcus* and haptophyte *rbcL* RNA also showed statistically significant relationships with pCO_2, but with *R*-values of -0.584 and -0.630, respectively, neither had as strong a relationship as that from the heterokont group and high-light *Prochlorococcus*. *rbcL* RNA concentrations measured by dot-blot hybridization also showed strong negative relationships to pCO_2: forms IA ($r=-0.8484$), IB ($r=-0.9241$) and ID ($r=-0.8831$). However, the actual concentrations of forms IA and IB were much lower than those of form ID, which paralleled heterokont *rbcL* RNA trends from station to station (Supplementary Data).

Figure 6 highlights the differing nature of the relationship between high-light *Prochlorococcus* and heterokont *rbcL* RNA with pCO_2. Essentially two regimes existed with respect to pCO_2 levels: plume stations where pCO_2 was below atmospheric concentrations and an estimated influx of CO_2

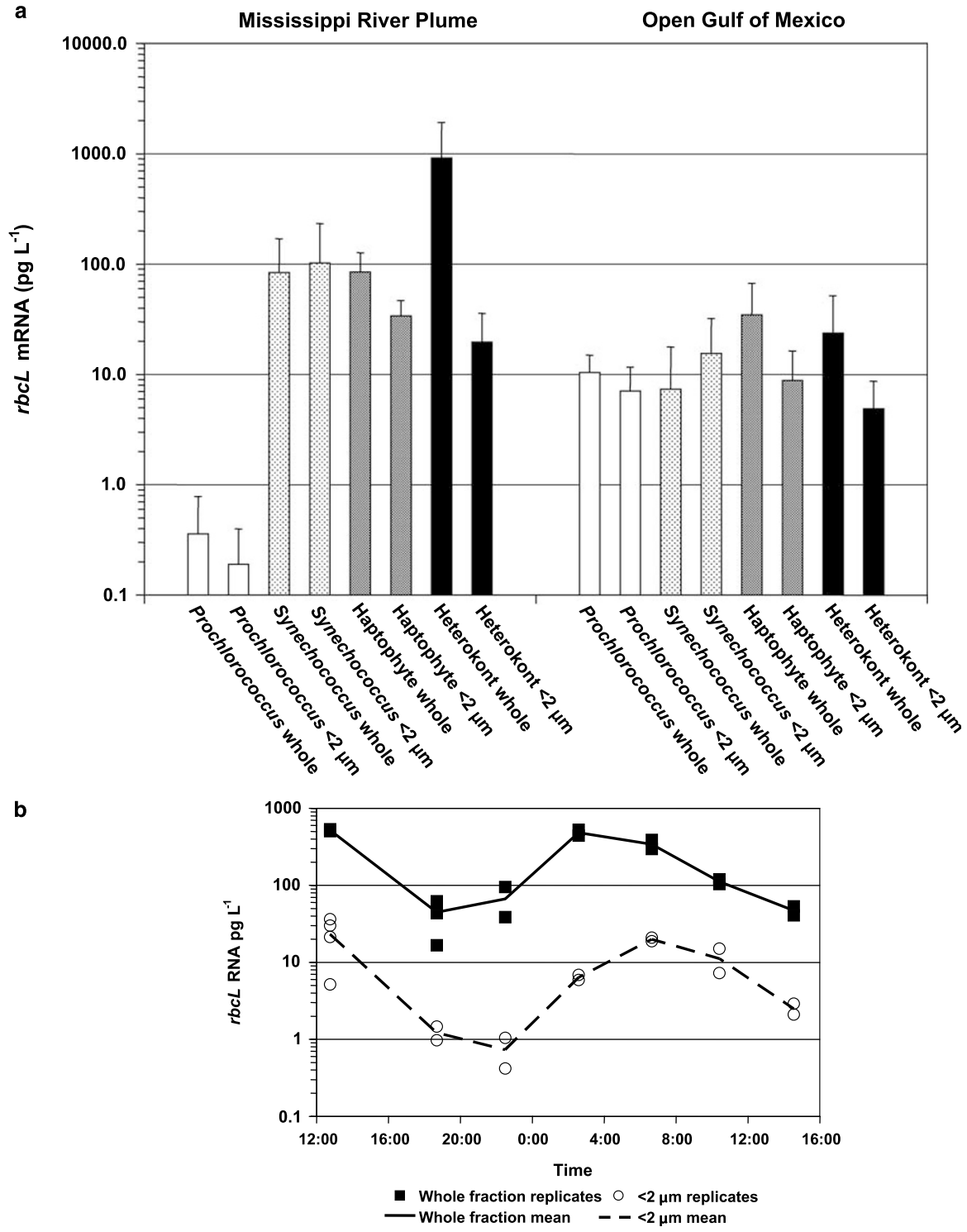

Figure 4 (**a**) Average *rbcL* RNA concentrations per liter of the four groups measured by qPCR, in the whole (unfiltered) and $<2\,\mu m$ size fractions. Replicate samples from the multiple stations are included. Means are grouped by MRP (salinity 30–32) and open Gulf of Mexico (salinity >34) stations. The heterokont group detects *rbcL* RNA from diatoms, pelagophytes, dictyochophytes (silicoflagellates) and pinguiophytes, which have closely related *rbcL* genes. Only high-light *Prochlorococcus* are detected by the qPCR assay. Error bars show standard deviation. Only samples taken from 0600 to 1300 hours are included, which is all except Station 4 and three diel time points (see Table 1). (**b**) Diel cycle *rbcL* RNA concentrations per liter from the heterokont group in whole and $<2\,\mu m$ size fractions, measured by qPCR. Other groups diel cycles shown in Supplementary Data. Behind the diel trend, there appeared to be mixing with lower productivity water, as indicated both by the difference between consecutive 1200 time points here and decreasing chlorophyll-*a* measurements over the course of the diel sampling (1.86–0.80 $\mu g\,l^{-1}$, Table 1). MRP, Mississippi River plume; qPCR, quantitative PCR.

Table 2 Highlights of relationships among data sets indicated by Pearson correlation coefficients (*R*)

Parameters compared	*Correlation coefficient (*R*)*	n	*Significance of regression (*P < *x)*
Seawater rbcL RNA concentrations and cell counts			
Log diatom cells vs log heterokont *rbcL* RNA (PCR)	0.98	12	1.0E−08
Log auto- and heterotrophic microflagellates cells vs log heterokont *rbcL* RNA (PCR)	0.77	14	0.002
Log sum of diatom+microflagellates vs log heterokont *rbcL* RNA (PCR)	0.96	14	1.0E−07
Log *Synechococcus* cells vs log *Synechococcus rbcL* RNA (PCR)	0.73	22	0.003
Log picoeukaryote phytoplankton <2 μm vs log <2 μm haptophyte *rbcL* RNA (PCR)	0.67	18	0.009
Log picoeukaryote phytoplankton <2 μm vs log <2 μm heterokont rbcL RNA (PCR)	0.42	18	0.09
Log *Prochlorococcus* cells vs log HL *Prochlorococcus rbcL* RNA (PCR)	0.60	18	0.01
Log dinoflagellate cells vs log form IB *rbcL* RNA (dot blot hyb.)	0.92	12	1.0E−04
Log *Prochlorococcus* cells vs log form IA RNA (dot-blot hybridization)	−0.72	16	0.002
Log *Synechococcus* cells vs log form IA RNA (dot-blot hybridization)	0.44	16	0.09
Productivity/chlorophyll concentrations and phytoplankton parameters			
Chlorophyll-*a* vs log heterokont *rbcL* RNA (PCR)	0.89	16	1.0E−05
P_{max} vs heterokont *rbcL* RNA (PCR)	0.72	16	0.003
P_{max} vs diatom cells	0.97	7	0.001
Seawater chemical parameters and phytoplankton/biological parameters			
Salinity vs log heterokont *rbcL* RNA (PCR)	−0.91	18	1.0E−06
Salinity vs log HL *Prochlorococcus rbcL* RNA (PCR)	0.86	18	1.0E−05
*p*CO2 vs log heterokont *rbcL* RNA (PCR)	−0.90	18	1.0E−05
*p*CO2 vs log HL *Prochlorococcus rbcL* RNA (PCR)	0.83	18	1.0E−04
pCO_2 vs log diatom cells	−0.89	7	0.01
pCO_2 vs log *Prochlorococcus* cells	0.46	12	*Not significant*
pCO_2 vs Chlorophyll-*a*	−0.88	12	0.001
pCO_2 vs P_{max}	−0.72	12	0.01
Other			
pCO_2 vs salinity	0.97	13	1.0E−07

All samples compared were from surface water (3 m). Comparisons involving *rbcL* RNA included data points from samples taken between 0600 and 1300 hours Eastern Daylight Time, to limit variability due to diel turnover of *rbcL* mRNA transcripts. HL *Prochlorococcus* = 'high-light' *Prochlorococcus*. Comparisons not involving RNA include all surface stations, except where data was not recorded (see Table 1).

occurred, and non-plume stations where seawater pCO_2 was moderately greater than atmospheric levels and a small efflux occurred. RuBisCO transcripts from the two groups also fall into these respective regimes, with the two essentially equal in non-plume stations and dramatically divergent in plume stations. A log-linear negative relationship between heterokont *rbcL* RNA and surface seawater pCO_2 is shown in Figure 6. The opposite relationship was observed for high-light *Prochlorococcus rbcL* RNA, which reveals a highly significant positive regression ($P < 0.0001$, $r^2 = 0.69$). Although the extremely low concentrations of *rbcL* RNA in the plume and lack of intermediate pCO_2 measurements between 300 and 400 μatm result in a distribution of *Prochlorococcus rbcL* RNA vs pCO_2 that does not appear linear, when the data are considered in light of plume vs open Gulf of Mexico samples, the difference between the two regimes is clear. RuBisCO RNA transcripts from *Synechococcus* and haptophytes did not show such a distribution as that from *Prochlorococcus* or the heterokont group with respect to pCO_2 (correlation coefficient *R*-values of 0.58 and 0.63, respectively).

Discussion

The surface water chemical characteristics measured allow us to categorize the sampling stations into 'plume' stations (those with salinities between 30 and 32 and pCO_2 under 310 μatm) and 'non-plume' stations (those with salinities greater than 34 and pCO_2 greater than 400 μatm). Our plume stations fall in the salinity range that other MRP papers characterize as a mixing zone, containing higher salinity than the water masses with greatest productivity (Lohrenz *et al*., 1999). Nonetheless, data from these stations provide a good evaluation of the relative trends of RuBisCO gene transcript concentrations among the evaluated phytoplankton groups in relation to surface CO_2 partial pressures.

The following pieces of evidence indicate that diatoms are the most important phytoplankton group whose productivity drives the CO_2 drawdown found in the MRP region. (1) We found an overwhelming dominance of heterokont *rbcL* transcripts quantified by real-time PCR in the plume stations, on average 10× greater than the next closest group (Figure 4a). Our heterokont PCR assay

detects diatom, pelagophyte, pinguiophyte, and most silicoflagellate *rbcL* transcripts with equal efficiency (John and Paul, 2007). (2) The heterokont *rbcL* RNA concentrations are negatively correlated to surface water pCO_2 levels (Figure 6). (3) The heterokont *rbcL* gene expression signal correlates very closely to diatom and the sum of diatom and microflagellate cell abundances, better than to microflagellates alone (Figure 5 and Table 2). (4) Among the microplankton counted by light microscopy, diatoms were in greatest numbers in the plume, except at Station 5, where microflagellates were equally numerous (Figure 3). It is not known which portion of these flagellates were photoautotrophs because of the method used for their enumeration. However, the importance of microflagellates in the composition of total 'heterokont' *rbcL* RNA abundances appears to be most important in the open, non-plume stations with very low numbers of diatoms. (5) Heterokont *rbcL* mRNA, diatom and microflagellate cell counts,

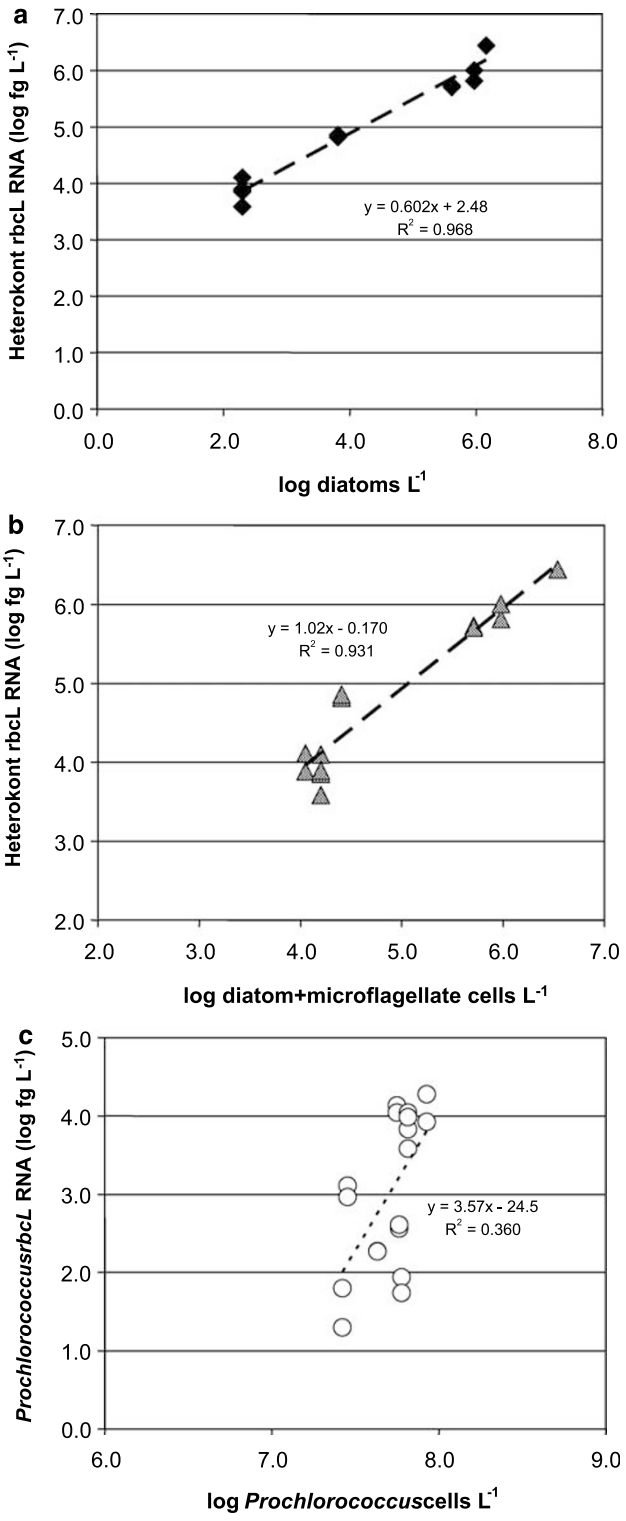

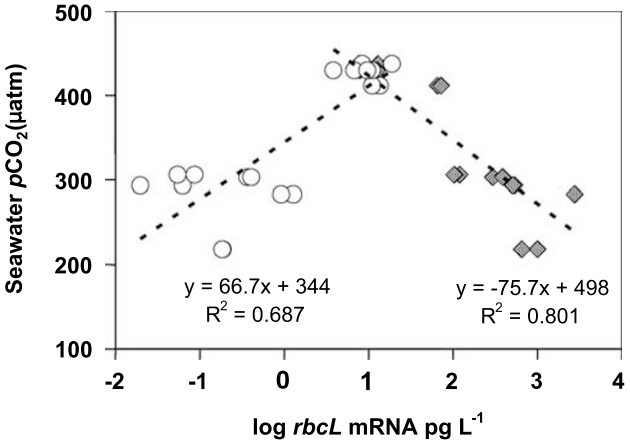

Figure 6 Correlation of *rbcL* mRNA concentrations to seawater pCO_2 for samples from 0600 to 1300 hours Eastern Daylight Time, showing heterokont (◇) and high-light *Prochlorococcus* (●) *rbcL* RNA concentrations, with log-linear regressions placed right and left, respectively. The divergence of data from plume and open Gulf of Mexico stations is apparent, in that outside the plume in higher pCO_2 water, the heterokont group and *Prochlorococcus rbcL* RNA concentrations are similar. In the plume, at lower pCO_2 $\leqslant$300 µatm, heterokont *rbcL* RNA abundance is dramatically greater than that of *Prochlorococcus*. The values for *Prochlorococcus* are extremely low, at the limits of detection for the qPCR assay, and are not resolved as accurately, thus giving rise to the observed spread along the low end of this logarithmic scale. qPCR, quantitative PCR.

Figure 5 Relationships between measured *rbcL* RNA concentrations per liter and cell counts for (**a**) heterokont *rbcL* RNA and diatoms, (**b**) heterokont *rbcL* RNA and the sum of diatoms and microflagellates, and (**c**) cell counts for *Prochlorococcus* cells and high-light *Prochlorococcus rbcL* RNA. The figures depict data from samples taken from 0600 to 1300 hours only. On (**b**), diatoms make up the larger fraction of the sum in plume stations (those on the higher end of the scale), while microflagellates compose most or all of the sum from oligotrophic open Gulf of Mexico stations (on the lower end of distribution). For *Prochlorococcus* (**c**), the clustering among samples from plume stations and those outside the plume is apparent, with the open Gulf of Mexico samples having greater than $1 \times 10^{3.5}$ fg *rbcL* RNA per liter. All the values below this are from the MRP stations. MRP, Mississippi River plume.

chlorophyll-*a*, and pCO_2 all share strong correlations to each other (Table 2). (6) P_{max} values, a measure of primary productivity in the water mass, were best correlated to both the heterokont *rbcL* RNA abundance and diatom cell counts (Table 2). (7) Although picoeukaryotes were in considerably greater abundance than diatoms throughout the sampling region, including the MRP, they were principally in the $<2\,\mu m$ size fraction (Supplementary data), that only represented a small fraction ($\sim 2\%$) of the heterokont *rbcL* mRNA signal (Figures 3 and 4). Also, the heterokont *rbcL* signal is poorly correlated to the picoeukaryote cell abundance (Table 2). (8) Plume *Synechococcus rbcL* RNA concentrations were much lower than those of the heterokont group, in spite of the high *Synechococcus* cell counts, and were not well correlated to seawater pCO_2 data (Figures 3 and 4a).

This evidence thus supports our conclusion that ($>2\,\mu m$) eukaryotes, particularly diatoms, were responsible for the carbon fixation and CO_2 drawdown we and others (Cai, 2003; Lohrenz and Cai, 2006) have observed in the MRP, and not picoplankton such as *Synechococcus* or picoeukaryotes which exist in much greater numbers throughout the plume area. Our findings also support the existing paradigm of MRP phytoplankton community dynamics, which dictates that production led by diatoms is prevalent in the mid-salinity plume where river water mixes with the Gulf of Mexico (Bode and Dortch, 1996; Lohrenz *et al.*, 1999; Liu and Dagg, 2003; Liu *et al.*, 2004; Wawrik and Paul, 2004; Wawrik *et al.*, 2004).

In contrast to the observations of the heterokont group's *rbcL* expression, levels of high-light *Prochlorococcus rbcL* mRNA decreased dramatically with reduced pCO_2 partial pressure. *Prochlorococcus rbcL* RNA was not even detectable at Station 4 with the lowest pCO_2, in spite of a very low limit of detection for this assay, which is in the order of 1–10 total copies; we also note that this may partially be due to the late-day sampling time. Yet, compared to the variability of high-light *Prochlorococcus rbcL* RNA, *Prochlorococcus* cell counts varied relatively little. The difference in mean *rbcL* RNA concentration (per liter) is about 25-fold between oligotrophic stations and plume stations (Figure 4a) and the total range is over 1000-fold (Figure 5c). However, *Prochlorococcus* cell counts varied only by a factor of about three, being greater outside the plume. If the amount of *rbcL* RNA per *Prochlorococcus* cell is estimated, those outside the plume contained an average of over 14 $\times$ more *rbcL* RNA per cell, all else being equal.

It is possible that *Prochlorococcus* cells observed in plume expressed a variant of *rbcL* not detected by our PCR assay probe and primers. However, form IA *rbcL* RNA detected by probe hybridization apparently did not provide an indication of *Prochlorococcus* activity in the plume either, based on the very poor correlation to cell numbers, and it is unlikely that these would be low-light *Prochlorococcus* ecotypes since samples were taken from 3 m. We hypothesize that the *Prochlorococcus* populations in the plume are in an inactive state, possibly the result of advection into low salinity and high nutrient water. Form IA *rbcL* transcripts measured by dot-blot hybridization (Supplementary data) decrease with higher salinity, and appear to represent gene expression from non-*Prochlorococcus* and *Synechococcus* organisms, perhaps that of chemolithotrophic bacteria. Others have described high rates of nitrification in mid-salinity MRP water (Pakulski *et al.*, 1995); nitrifying chemoautotrophic bacteria may be responsible for much of the form IA *rbcL* detected by hybridization. It may also be that form IA *rbcL* RNA values were influenced by cross-hybridization to form IB or the highly abundant form ID transcripts present. Given the very large differences in concentrations, even a small degree of cross-hybridization would skew apparent form IA *rbcL* RNA values.

The evidence we present here supports the concept that diatoms, and possibly other chromophytic eukaryotes such as pelagophytes (that is, at Station 5), are able to capitalize most effectively on the high levels of nutrients input to the surface waters of the northern Gulf of Mexico by the Mississippi River, and maintain a high rate of carbon fixation under situations of depressed pCO_2 in these productive ocean waters. To succeed in such situations, blooming marine phytoplankton populations must be able to rapidly utilize the available nitrogen input, tolerate the reduced salinity and light conditions, maintain adequate intracellular inorganic carbon stores, and reproduce quickly enough to offset zooplankton grazing. Liu and Dagg (2003) have found evidence of saturated zooplankton grazing on phytoplankton in the 5–20 μm and $>20\,\mu m$ fractions, but not on the 'ultra' fraction ($<5\,\mu m$) in the Mississippi River plume, suggesting that microzooplankton are better able to control $<5\,\mu m$ phytoplankton populations. This may partially explain the 'success' of diatoms in the Mississippi River plume. However, it is unknown how this would apply to even smaller organisms such as *Synechococcus* and *Prochlorococcus*.

Flow cytometer and microscopic counts performed for our study revealed numbers of cyanobacteria and picoeukaryotes much greater than the larger diatoms and microflagellates (by 10- to 100-fold). Yet, *rbcL* RNA concentrations corresponding to cyanobacteria were much lower in the plume than for the $>2\,\mu m$ heterokont group (by 10- to 100-fold). Naturally, due to their size, the amount of RubisCO RNA and carbon fixation potential per cyanobacteria or picoeukaryote cell would be less than the larger eukaryotic phytoplankton. But differential grazing rates would not explain the disconnect between *Prochlorococcus* cell numbers and *rbcL* RNA concentrations between plume and non-plume stations

(the estimated 14 × greater amount of *rbcL* RNA per *Prochlorococcus* cell outside the plume).

One hypothesis that merits further investigation is whether the success of some phytoplankton in highly productive nutrient plumes is enabled by efficient carbon concentrating mechanisms (CCMs). Diatoms have been shown to possess multiple CCMs and an ability to regulate active inorganic carbon uptake under conditions of reduced CO_2 (Giordano *et al.*, 2005). These CCMs include external (periplasmic) carbonic anhydrases, which convert HCO_3^-, generally the dominant inorganic carbon species in marine water, into CO_2 which is more readily transported across the cell membrane, and inducible active CO_2 and HCO_3^- transport mechanisms (Burkhardt *et al.*, 2001; Matsuda *et al.*, 2001). *Prochlorococcus*, which are adapted to oligotrophic environments with DIC concentrations of at least 2 mM, as in our non-plume stations, apparently have limited CCM capabilities, particularly the high-light *Prochlorococcus* with their highly reduced genomes (Badger and Price, 2003; Badger *et al.*, 2006). Their inability to enhance inorganic carbon uptake under the reduced pCO_2 levels found in more productive waters may be a significant reason they cannot sustain carbon fixation, resulting in reduced *rbcL* transcription. Thus, we present a conceptual model on the relationship of freshwater input, CCMs, phytoplankton community dynamics, and marine carbon dynamics in the MRP and possibly other river plumes: nutrient-laden freshwater mixes with the Gulf of Mexico, larger phytoplankton such as diatoms capitalize and grow rapidly in the mid-salinity waters as turbidity decreases, while efficient CCMs allow sustained carbon fixation in the face of reduced external pCO_2. The result is surface ocean CO_2 drawdown and regional flux of atmospheric CO_2 to the sea. *Prochlorococcus* cells, which were possibly carried into the mixing area on the southern fringe of the MRP from oligotrophic regions by the Loop Current, are unable to sustain carbon fixation in the low CO_2 water due to relatively inefficient uptake, possibly compounded by increased turbidity, excessive nutrients, and low salinity, and enter a relatively senescent state of low *rbcL* gene expression.

These results constitute the first attempts to describe relationships between carbon fixation gene expression among phytoplankton communities and oceanic/atmosphere CO_2 fluxes. Molecular methods such as we present here have the potential to be employed more rapidly and with higher throughput as biotechnology platforms such as PCR arrays or *in situ* genosensors develop. The underlying intent for our measurement of carbon fixation gene expression markers from environmental samples is to provide a phylogenetically specific indication of productivity, or at least its potential, from the microbial community present. Covariance between the heterokont group *rbcL* mRNA concentrations and carbon fixation (as P_{max}) was less robust than with pCO_2 or chlorophyll concentrations. A regression of samples taken from 0600 to 1300 hours shows a significant relationship ($P = 0.003$) but an r^2 of only 0.48. Perhaps due to the complexity of RuBisCO activity regulation, ecosystem dynamics, and offset temporal cycles, quantitative relationships between environmental *rbcL* transcript levels and net primary productivity or photosynthetic rates have not always been easy to resolve. Nonetheless, meta-analysis using results from several different studies reveals a good overall correlation between *rbcL* transcript abundances and carbon fixation (as either net primary productivity or maximum photosynthetic potential [P_{max}]) on a logarithmic scale, with an r^2 of 0.602, highly significant at $P < 0.00001$ (Figure 7, with data from this paper, Wawrik *et al.*, 2002, 2003, 2004; Corredor *et al.*, 2004).

Measurement of *rbcL* mRNA from the environment appears to be good for characterizing large-scale differences found among differing oceanic environments such as river plumes and other coastal areas with the open ocean, and for determining the active carbon-fixing organisms based on gene sequence specificities. The current techniques still require refinement, particularly enhancing phylogenetic specificity of heterokont oligonucleotides to differentiate between diatoms, pelagophytes, and other chromophytes, and development of additional assays for important phytoplankton such as various prasinophytes, low-light *Prochlorococcus*, autotrophic dinoflagellates, and even some HAB-forming species. Still, analyses of this type continue to show promise, and with the use of real-time PCR for RNA, we can achieve an unsurpassed level of

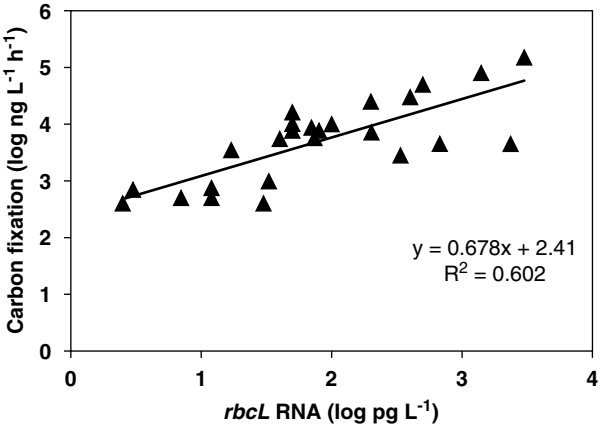

Figure 7 Relationship of measured carbon fixation, as net primary productivity or maximum photosynthetic potential (P_{max}), to *rbcL* mRNA from dominant form or *rbcL* type measured. Data from (Wawrik *et al.*, 2002, 2003, 2004; Corredor *et al.*, 2004); this study. Sample locations were Gulf of Mexico and mid-Atlantic coast of United States (LEO-15, (Corredor *et al.*, 2004)). *rbcL* data were from form IA hybridization analyses (Wawrik *et al.*, 2003, 2004) or heterokont quantitative reverse transcription PCR assay originally described in Wawrik *et al.* (2002) and used for data from that paper (Corredor *et al.*, 2004), and adapted assay used for this study.

quantitative sensitivity and specificity. Continued development and application of gene expression techniques will hopefully enable enhanced understanding of the underlying physiologic mechanisms regulating community dynamics and important ecological phenomena such as carbon flux and marine productivity.

Acknowledgements

We acknowledge the assistance of Gabriel Vargo for phytoplankton microscopic counts and Lisa Campbell for flow cytometry, Brian Witte, Brian Zielinski, Stacey Patterson, Lauren McDaniel, Jennifer Mobberley, Michele de la Rosa and Erica Casper for field and laboratory assistance. We also acknowledge the assistance of the crew of the *M/V Pelican* (LUMCON). This research was supported by the Office of Science (BER), US Department of Energy, Grant No. DE-FG02-97ER62452. Ship time was funded by NSF Grant OCE-0221763.

References

Badger MR, Price GD. (2003). CO_2 concentrating mechanisms in cyanobacteria: molecular components, their diversity and evolution. *J Exp Bot* **54**: 609–622.

Badger MR, Price GD, Long BM, Woodger FJ. (2006). The environmental plasticity and ecological genomics of the cyanobacterial CO_2 concentrating mechanism. *J Exp Bot* **57**: 249–265.

Behrenfeld MJ, Randerson JT, McClain CR, Feldman GC, Los SO, Tucker CJ *et al.* (2001). Biospheric primary production during an ENSO transition. *Science* **291**: 2594–2597.

Bode A, Dortch Q. (1996). Uptake and regeneration of inorganic nitrogen in coastal waters influenced by the Mississippi River: spatial and seasonal variations. *J Plankton Res* **18**: 2251–2268.

Burkhardt S, Amoroso G, Riebesell U, Sultemeyer D. (2001). CO_2 and HCO_3—uptake in marine diatoms acclimated to different CO_2 concentrations. *Limnol Oceanogr* **46**: 1378–1391.

Byrne RH, Liu XW, Kaltenbacher EA, Sell K. (2002). Spectrophotometric measurement of total inorganic carbon in aqueous solutions using a liquid core waveguide. *Anal Chim Acta* **451**: 221–229.

Cai WJ. (2003). Riverine inorganic carbon flux and rate of biological uptake in the Mississippi River plume. *Geophys Res Lett* **30**: Art No. 1032.

Campbell L. (2001). Flow cytometric analysis of autotrophic picoplankton. In: Paul JH (ed). *Marine Microbiology, Methods in Microbiology*, vol. 30. Academic Press: San Diego, pp 317–343.

Corredor JE, Wawrik B, Paul JH, Tran H, Kerkhof L, Lopez JM *et al.* (2004). Geochemical rate-RNA integrated study: ribulose-1,5-bisphosphate carboxylase/oxygenase gene transcription and photosynthetic capacity of planktonic photoautotrophs. *Appl Environ Microbiol* **70**: 5459–5468.

Dagg M, Benner R, Lohrenz S, Lawrence D. (2004). Transformation of dissolved and particulate materials on continental shelves influenced by large rivers: plume processes. *Cont Shelf Res* **24**: 833–858.

Dodson AN, Thomas WH. (1978). Monographs on oceanographic methodology no. 6. In: Sournia A (ed). *Phytoplankton Manual*. UNESCO: Paris, pp 104–107.

Giordano M, Beardall J, Raven JA. (2005). CO_2 concentrating mechanisms in algae: mechanisms, environmental modulation, and evolution. *Annu Rev Plant Biol* **56**: 99–131.

Green RE, Bianchi TS, Dagg MJ, Walker ND, Breed GA. (2006). An organic carbon budget for the Mississippi River turbidity plume and plume contributions to air-sea CO_2 fluxes and bottom water hypoxia. *Estuaries Coasts* **29**: 579–597.

Hartman FC, Harpel MR. (1994). Structure, function, regulation, and assembly of D-Ribulose-1,5-bisphosphatecarboxylase oxygenase. *Annu Rev Biochem* **63**: 197–234.

Huertas E, Navarro G, Rodriguez-Galvez S, Prieto L. (2005). The influence of phytoplankton biomass on the spatial distribution of carbon dioxide in surface sea water of a coastal area of the Gulf of Cadiz (Southwestern Spain). *Can J of Bot—Revue Canadienne De Botanique* **83**: 929–940.

Jochem FJ. (2003). Photo- and heterotrophic pico- and nanoplankton in the Mississippi River plume: distribution and grazing activity. *J Plankton Res* **25**: 1201–1214.

John DE, Paul JH. (2007). Phytoplankton-group specific quantitative PCR Assays for rubisco gene expression in seawater. *Mar Biotechnol* (doi:10.1007/s10126-007-9027-z).

Liu HB, Dagg M. (2003). Interactions between nutrients, phytoplankton growth, and micro- and mesozooplankton grazing in the plume of the Mississippi River. *Mar Ecol Prog Ser* **258**: 31–42.

Liu HB, Dagg M, Campbell L, Urban-Rich J. (2004). Picophytoplankton and bacterioplankton in the Mississippi River plume and its adjacent waters. *Estuaries* **27**: 147–156.

Lohrenz SE, Cai WJ. (2006). Satellite ocean color assessment of air-sea fluxes of CO_2 in a river-dominated coastal margin. *Geophys Res Lett* **33**: Art No. L01601.

Lohrenz SE, Fahnenstiel GL, Redalje DG, Lang GA, Dagg MJ, Whitledge TE *et al.* (1999). Nutrients, irradiance, and mixing as factors regulating primary production in coastal waters impacted by the Mississippi River plume. *Cont Shelf Res* **19**: 1113–1141.

Matsuda Y, Hara T, Colman B. (2001). Regulation of the induction of bicarbonate uptake by dissolved CO_2 in the marine diatom, *Phaeodactylum tricornutum*. *Plant Cell Environ* **24**: 611–620.

Pakulski JD, Benner R, Amon R, Eadie B, Whitledge T. (1995). Community metabolism and nutrient cycling in the Mississippi River plume—evidence for intense nitrification at intermediate salinities. *Mar Ecol Prog Ser* **117**: 207–218.

Paul JH, Alfreider A, Kang JB, Stokes RA, Griffin D, Campbell L *et al.* (2000a). Form IA rbcL transcripts associated with a low salinity/high chlorophyll plume ('Green River') in the eastern Gulf of Mexico. *Mar Ecol Prog Ser* **198**: 1–8.

Paul JH, Kang JB, Tabita FR. (2000b). Diel patterns of regulation of rbcL transcription in a cyanobacterium and a prymnesiophyte. *Mar Biotechnol* **2**: 429–436.

Paul JH, Pichard SL, Kang JB, Watson GMF, Tabita FR. (1999). Evidence for a clade-specific temporal and

spatial separation in ribulose bisphosphate carboxylase gene expression in phytoplankton populations off Cape Hatteras and Bermuda. *Limnol Oceanogr* **44**: 12–23.

Pichard SL, Campbell L, Kang JB, Tabita FR, Paul JH. (1996). Regulation of ribulose bisphosphate carboxylase gene expression in natural phytoplankton communities.1. Diel rhythms. *Mar Ecol Prog Ser* **139**: 257–265.

Platt T, Sathyendranath S, Ravindran P. (1990). Primary production by phytoplankton—analytic solutions for daily rates per unit area of water-surface. *Proc R Soc Lond, B* **241**: 101–111.

Sabine CL, Heiman M, Artaxo P, Bakker D, Chen C, Field CB *et al.* (2004). Current status and past trends of the carbon cycle. In: Field CB, Raupach MR (eds). *The Global Carbon Cycle: Integrating Humans, Climate, and The Natural World. SCOPE 62*. Island Press: Washington, DC, pp 17–46.

Tabita FR. (1995). The biochemistry and metabolic regulation of carbon metabolism and CO_2 fixation in purple bacteria. In: Blankenship RE, Madigan MT, Bauer CE (eds). *Anoxygenic Photosynthetic Bacteria*. Kluwer Publishers: Dordrecht, the Netherlands, pp 885–914.

Tabita FR. (1999). Microbial ribulose 1,5-bisphosphate carboxylase/oxygenase: a different perspective. *Photosynth Res* **60**: 1–28.

Thomas H, Bozec Y, Elkalay K, de Baar HJ. (2004). Enhanced open ocean storage of CO_2 from shelf sea pumping. *Science* **304**: 1005–1008.

Tomas C. (1997). *Identifying Marine Phytoplankton*. Academic Press: San Diego.

Wang ZA, Liu X, Byrne RH, Wanninkhof R, Bernstein RE, Kaltenbacher EA *et al.* (2007). Simultaneous spectrophotometric flow-through measurements of pH, carbon dioxide fugacity, and total inorganic carbon in seawater. *Anal Chim Acta* **596**: 23–36.

Wanninkhof R. (1992). Relationship between wind-speed and gas-exchange over the ocean. *J Geophys Res C* **97**: 7373–7382.

Wawrik B, Paul JH. (2004). Phytoplankton community structure and productivity along the axis of the Mississippi River plume in oligotrophic Gulf of Mexico waters. *Aquat Microb Ecol* **35**: 185–196.

Wawrik B, Paul JH, Bronk DA, John D, Gray M. (2004). High rates of ammonium recycling drive phytoplankton productivity in the offshore Mississippi River plume. *Aquat Microb Ecol* **35**: 175–184.

Wawrik B, Paul JH, Campbell L, Griffin D, Houchin L, Fuentes-Ortega A *et al.* (2003). Vertical structure of the phytoplankton community associated with a coastal plume in the Gulf of Mexico. *Mar Ecol Prog Ser* **251**: 87–101.

Wawrik B, Paul JH, Tabita FR. (2002). Real-time PCR quantification of rbcL (ribulose-1,5-bisphosphate carboxylase/oxygenase) mRNA in diatoms and pelagophytes. *Appl Environ Microbiol* **68**: 3771–3779.

Welschmeyer NA. (1994). Fluorometric analysis of chlorophyll-*a* in the presence of chlorophyll-B and pheopigments. *Limnol Oceanogr* **39**: 1985–1992.

Wyman M. (1999). Diel rhythms in ribulose-1,5-bisphosphate carboxylase/oxygenase and glutamine synthetase gene expression in a natural population of marine picoplanktonic cyanobacteria (*Synechococcus* spp.). *Appl Environ Microbiol* **65**: 3651–3659.

Wyman M, Davies JT, Crawford DW, Purdie DA. (2000). Molecular and physiological responses of two classes of marine chromophytic phytoplankton (diatoms and prymnesiophytes) during the development of nutrient-stimulated blooms. *Appl Environ Microbiol* **66**: 2349–2357.

Supplementary Information accompanies the paper on The ISME Journal website (http://www.nature.com/ismej)